Reprinted from the Journal of The American Ceramic Society, Vol. 58, No. 9-10 September-October 1975

Strength Degradation of Brittle Surfaces: Blunt Indenters

B. R. LAWN,† S. M. WIEDERHORN,* and H. H. JOHNSON

Institute for Materials Research, National Bureau of Standards, Washington, DC 20234

Indentation fracture mechanics is used to develop a theoretical basis for predetermining the strength properties of brittle surfaces in prospective contact situations. Indenters are classified as blunt or sharp; only the first is considered in the present work. The classical Hertzian cone crack conveniently models the fracture damage incurred by the surface in this class of indentation event. Significant degradation is predicted at a critical contact load; when the load is increased beyond this critical level, further degradation occurs at a relatively slight rate. Bend tests on abraded glass slabs confirm the essential features of the theoretical predictions. The controlling variables in the degradation process, notably starting flaw size and indenter radius, are investigated systematically. An indication is also given as to optimization of material parameters.

I. Introduction

STRENGTH degradation of a brittle surface resulting from contact with a hard particle, especially in an impact situation, is an important consideration in ceramic engineering. A typical contact event may not, in itself, cause the failure of a structural component, but may nevertheless generate highly localized stresses of intensity sufficient to develop potentially dangerous cracks. With variables relating to particle geometry, loading conditions (e.g. loading rate), mechanical properties of the materials, state of the brittle surface, etc. complicating the general issue, it is little wonder that a fundamental description of the problem has been slow in evolving.

However, the emergence of the field of indentation fracture mechanics, recently reviewed by Lawn and Wilshaw,[1] establishes the necessary foundation for a theoretical analysis of contact-induced degradation. Evans[2] was the first to propose a theory along these lines, but his treatment addressed only one specific situation, i.e. impact loading with a hard spherical indenter, and did not explore the role of many important indentation variables. The present work was initiated in an effort to generalize the Evans analysis. The philosophy adopted here is that the strength properties of a material should be predictable from basic fracture parameters as determined from standard indentation tests.

To this end it is convenient, following the scheme of Ref. 1, to distinguish 2 distinct types of indenter: (1) blunt indenters (e.g. a hard sphere), characterized by a perfectly elastic contact such that crack initiation is controlled by preexisting flaws (usually at the specimen surface) and (2) sharp indenters (e.g. a cone or pyramid), characterized by a partially plastic contact such that the starting flaws are produced by the indentation process itself. Real contact situations may then be viewed as lying somewhere between these 2 limits. Only blunt indenters are discussed in the present paper; the investigation of sharp indenters is deferred to a subsequent publication. For simplicity, crack growth is considered to occur under quasi-static conditions throughout, an assumption that should hold for contact rates up to an appreciable fraction of sonic velocities.

II. The Spherical Indenter and Hertzian Cone Fracture

The nature of the cracking that results from the contact between an elastic sphere (indenter) and an elastic-brittle surface (specimen) is considered. This is the most widely used test configuration of classical Hertzian contact.[1] The elastic field, although complex, remains well-defined up to a critical load, at which point a cone-shaped crack suddenly develops in the specimen. Initiation of the cone crack invariably takes place at a pre-existing surface flaw located just outside the contact circle, where the tension is greatest. Figure 1 indicates the basic test parameters.

The mechanics of cone extension through the inhomogeneous Hertzian field has been investigated in great detail, both theoretically and experimentally.[3-10] For the purpose of strength evaluation, one must know how the size of the cone crack varies with indenter load. It is convenient to consider separately the behavior prior to and subsequent to critical loading.

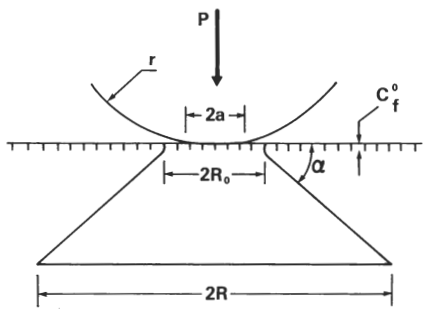

Fig. 1. Hertzian cone crack parameters.

(1) Subcritical Loading ($P \leq P_c$)

As the indenter load P steadily increases from its initial zero value, the ultimate starting flaw will experience a tensile stress field of growing intensity. In the absence of kinetic effects in crack growth, the condition for the sudden development of the surface flaw into a propagating cone may be readily formulated in terms of the fundamental, equilibrium energy-balance criterion of Griffith[11]: essentially, the cone develops when the crack-extension force associated with the applied loading exceeds the resistance term associated with the creation of new surface area. Because of the strong inhomogeneity of the Hertzian field, it is no simple matter to derive a single, exact analytical relation for the critical load as a function of starting flaw size. However, one can obtain working expressions for the limiting cases of small and large flaws[1,3]:

(A) Small Flaws: When surface flaws of effective initial length c_f^0 are very small in comparison with the scale of the elastic field (typically, $c_f^0 << 0.01\,a$, where a is the contact radius[3]), the gradient of stress along the crack trajectory may be considered to be negligibly small. In other words, a very small flaw will tend to respond as if it were located in a field of uniform tension. Thus, when the tensile strength of the material is exceeded at the site of the flaw (i.e. $K > K_{IC}$), unstable crack propagation ensues, and the cone accordingly develops spontaneously until a position of stability is once more attained remote from the contact area. On the assumption that initiation is favored at the surface location of maximum tensile stress, i.e. at the contact circle, the Hertzian equations predict[1,3,5,6]

$$P_c = \Gamma^{3/2} k^2 r^2 / \chi(\nu) E^{1/2} (c_f^0)^{3/2} \qquad (c_f^0 << 0.01a) \qquad (1)$$

where Γ is the fracture surface energy, $k = (9/16)[(1-\nu^2) + (1-\nu'^2)E/E']$ is a dimensionless constant, ν is Poisson's ratio, E is Young's modulus (the primes referring to the indenter material), r is the sphere radius, and $\chi(\nu) = \{(3/4)[3(1-\nu^2)(1-2\nu)^2/32\pi]^3\}^{1/2}$ is another dimensionless constant. Note, in particular, the dependence of the critical load on flaw size and ball radius.

(B) Large Flaws: For flaws sufficiently large that the (negative) gradient of tensile stress along their length becomes appreciable (typically, $c_f^0 \gtrsim 0.01\,a$), the approximation of a uniform field is no longer valid. Instead, there is a tendency to limited initial growth of the flaw as a stable surface ring just prior to cone formation.[3,7] That is, the crack must first surmount an energy barrier before it can become unstable; the conditions necessary for this behavior may, again, be evaluated from the Hertzian equations[1,3-6]

Received February 18, 1975; revised copy received April 26, 1975.
Supported by the U.S. Office of Naval Research under Contract No. NR-032-535.
*Member, the American Ceramic Society.
†On study leave from the School of Physics, University of New South Wales, Kensington, NSW, Australia.

$$P_c = 2\Gamma kr/\phi^*(\nu) = Ar \qquad (c_f^0 \gtrsim 0.01a) \qquad (2)$$

where $\phi^*(\nu)$ is another dimensionless constant whose value can be estimated (but only to within an order of magnitude) by numerical analysis, and A (Auerbach's constant) is a material constant named for the discoverer of the empirical "law" $P_c \propto r$.[12] The dependence of the critical load (P_c) on ball size is, therefore, less marked in the large-flaw region. The same is true of the dependence on flaw size; indeed, c_f^0 has no direct influence on P_c at all in Eq. (2).

The predictions of Eqs. (1) and (2) are represented in Fig. 2. In reality, the transition between the 2 regions of behavior is not as sharply defined as the analysis just given would suggest. This is indicated in Fig. 2 by means of an experimental curve, evaluated from some data on glass.[9] (These data, and indeed the data described in the present work, will fall more within the realm of Eq. (2) than of Eq. (1).) Accordingly, the theory will generally underestimate the true value of P_c, so that our ultimate estimates of strength will be on the conservative side.

Throughout the subcritical stage, $P < P_c$; therefore, little or no degradation of the brittle surface is expected. It is true that limited stable extension of surface flaws might occur just before critical loading, but any such extension is predicted to be imperceptibly small,[3] and will tend to be obscured in the general variation of flaw sizes sampled in the typical strength test.

(2) Supercritical Loading ($P > P_c$)

Once the critical load is exceeded, the crack grows substantially (typically, $R > 2a$ (Fig. 1)). For the limiting case of a true cone (i.e. $R_0 \rightarrow 0$) the mechanics of fracture become independent of events within the contact zone (i.e. of r and c_f^0), as seen in the simple equilibrium relation obtained by Roesler,[10]

$$P^2/R^3 = 2\Gamma E/\kappa_R(\nu) \qquad (R >> R_0) \qquad (3)$$

where $\kappa_R(\nu)$ is a dimensionless term which can be computed (to within a factor of ≈ 2) by numerical methods.[1] Evans[2] and others have analyzed more general cone configurations, but the expressions derived tend to be unwieldy. Moreover, the Roesler formula underestimates the indenter load necessary to maintain the cone at a prescribed depth, thus the present strength estimates will once again be conservative ones.

III. Strength Degradation Tests

The strength of a brittle solid is defined in terms of the applied stress required to break a test piece in uniform tension. From the Griffith energy-balance condition one obtains the standard expression

$$\sigma = [2\Gamma E/\pi(1-\nu^2)c_f]^{1/2} \qquad (4)$$

where σ is the applied stress and c_f is the effective length of the dominant flaw. This is an equilibrium expression involving material properties and surface state. The strength will accordingly be reflected somewhat in the microstructural influence on Γ (possibly also on E), but to a much greater degree in the influence of a wide range of past mechanical, thermal, and chemical events on c_f. Most ceramic surfaces contain a diversity of surface flaws up to 10 μm deep in even carefully handled test pieces; it is the largest of these flaws which determines the strength.

Since the prime concern in the present work is a systematic investigation of the factors affecting the mechanics of degradation, all strength tests were conducted under controlled surface conditions after the manner of Mould and Southwick.[13,14] Soda-lime glass was selected as a test material, mainly because of the availability of reliable data on its fracture properties[1,15] but also for reasons of economy, mechanical isotropy, and absence of microstructural complications. The test pieces were laths 250 by 37.5 by 5.65 mm, suitable for fracture in 4-point bending with a major span of 204 mm and a minor span of 37.5 mm. A center spot ≈ 15 mm in diameter was grit-blasted with a given grade of SiC abrasive on each tension face prior to testing, thereby introducing a more or less uniform density of starting flaws for the ensuing fracture. By covering the abraded spot with a drop of paraffin oil immediately after the blast treatment, any effects of moisture-assisted slow crack growth during subsequent testing could be largely eliminated. The bulk of the specimens were indented within the abrasion area with a tungsten carbide sphere of prescribed radius, at a preselected load, before rupture in bending. The delay between grit-blasting and ultimate rupture never exceeded 4 h.

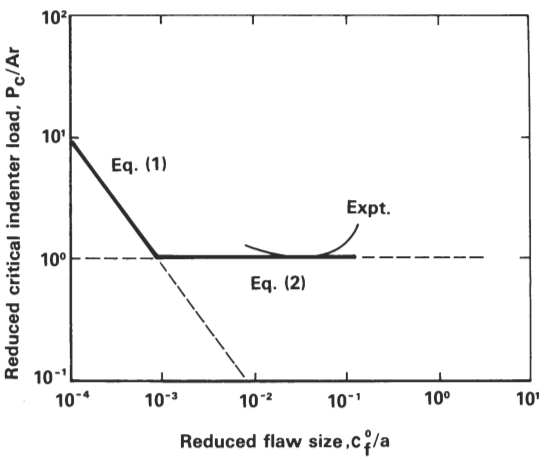

Fig. 2. Critical load to cone fracture as a function of starting flaw size. Limiting cases of Eqs. (1) and (2) shown as full, straight lines. (Controlling equation is that which predicts the larger value of P_c.) Real behavior shown as curve (note "tail" at large c_f^0 in real curve).

(1) Strength of Abraded Test Pieces

Strength tests were conducted on some nonindented specimens to establish the reproducibility of the grit-blast treatment and to determine the effective length of the flaws resulting from this treatment. In most cases the fracture could be unambiguously traced to an origin within the central abrasion spot, but a few isolated examples of premature edge failures were encountered; these latter were rejected from the data accumulation. Table I summarizes the results. The scatter in measured strengths for each grit size (usually $<10\%$) will be seen as small compared to the magnitude of the degradation effect to be investigated in Section III (2). The effective lengths of the abrasion flaws, $c_f = c_f^0$ (grit size), then follow from Eq. (4), using $E = 7.0 \times 10^{10}$ Nm^{-2}, $\nu = 0.25$ and $\Gamma = 3.9$ Jm^{-2} for glass.[15] Microscopic examination of the grit-blasted areas showed individual microcrack damage centers of dimensions consistent with those listed in Table I.[14]

(2) Strength of Indented Test Pieces

The effect of indentation load on strength was systematically investigated in a series of runs on glass specimens under conditions of given preabrasion treatment and sphere radius. In all such runs the strength remained essentially unaffected up to a critical indentation load, beyond which it declined steadily. This behavior is consistent with the theoretical description outlined earlier: for $P \leq P_c$ (Section II (1)), the effective length of the dominant flaw would be expected to hold constant at the characteristic size of the abrasion damage, i.e. $c_f = c_f^0$; similarly, for $P > P_c$ (Section II (2)), the effective flaw length would be expected to be governed by the geometry of the newly propagating cone crack, i.e. $c_f = c_f(R, \alpha)$ (Fig. 1). A more detailed analysis of the effectiveness of the conical crack as an initiating center for catastrophic failure in a tensile field can be given in terms of standard fracture-mechanics formulas

Table I. Strength* and Effective Flaw Size* of Grit-Blasted† Glass Test Pieces; Bend Tests in Oil Environment at a Crosshead Speed of 50 mm min^{-1}

Grade SiC grit	σ (MNm^{-2})	c_f^0 (μm)
100	79±7	23±5
150	86±4	19±3
200	94±7	16±3
240	107±9	12±2
320	123±5	10±1

*Mean value ± standard deviations ≥ 10 tests/run. †Air pressure = 0.275 MNm^{-2}.

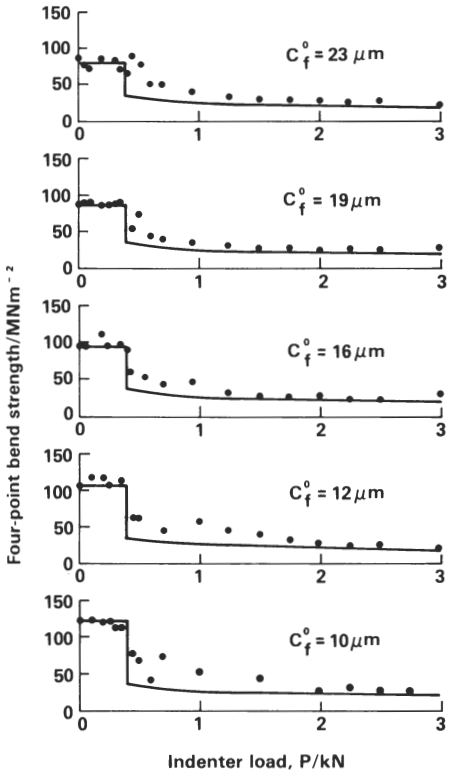

Fig. 3. Strength degradation as a function of indentation load for a given tungsten carbide sphere ($r=1.58$ mm) on soda-lime glass surfaces containing different abrasion flaw sizes (indicated). Oil environment. Crosshead speed for indentation tests was 0.5 mm min^{-1}, for bend tests, 50 mm min^{-1}.

(Appendix); at $R>>R_0$, $c_f=R\Omega(\alpha)$ is obtained where $\Omega(\alpha)$ is an angular-dependent dimensionless function (evaluated in the Appendix). Taken in conjunction with Eq. (3), this term gives the effective flaw size as a function of indentation load. The strength equation (Eq. (4)) accordingly becomes

$$\sigma=[2\Gamma E/\pi(1-\nu^2)c_f^0]^{1/2} \quad (P<P_c) \tag{5a}$$

$$\sigma=\{(2\Gamma E)^{2/3}/\Omega(\alpha)^{1/2}[\pi(1-\nu^2)]^{1/2}\kappa_R(\nu)^{1/6}\}P^{-1/3} \quad (P>P_c) \tag{5b}$$

These relations, together with Eqs. (1) and (2), provide, in principle, the basis for predetermining the degradation behavior without resorting to extensive (and, for all but the most common ceramic materials, expensive) failure testing under simulated service conditions.

Apart from the quantities E, ν, and Γ already specified, the information necessary for a complete evaluation of the present expressions may be obtained using straightforward indentation testing methods.[1] Typical values for a tungsten carbide sphere on a soda-lime glass specimen are as follows: $k=0.55$ and $\chi=5.1\times10^{-4}$ (calculable directly from the elastic constants); $\alpha=22\pm1°$ (from direct observation of the cone angle[3]), giving $\Omega=0.25\pm0.02$ (Appendix); $\phi=(1.7\pm0.2)\times10^{-5}$ (from tests on No. 320 grit-blasted glass in oil, $A=(390\pm35)$ N/1.58 mm, Eq. (2)); and $\kappa_R=(1.3\pm0.2)\times10^{-3}$ (from vacuum observations of fully developed cone crack[1]).* This leaves the abrasion flaw size c_f^0 and sphere radius r as convenient test variables for investigation here:

(A) Effect of Flaw Size: The first set of indentation/strength tests was conducted to investigate the role of initial flaw size on the ultimate strength degradation. The experimental results (data points) are compared with the theoretical predictions of Eq. (5) in Fig. 3 (full lines) for a sphere of $r=1.58$ mm. The following points of interest concern correlations in the different regions of behavior: (1) At $P<P_c$, there is no detectable degradation, as predicted (other than the usual deterioration associated with the increasing severity of the preabrasion treatment). (2) At $P=P_c$, the strength cutoff point is reasonably independent of the abrasion flaw size[5] (although small systematic deviations from constancy in P_c are apparent at the larger flaw sizes). This is consistent with behavior in the Auerbach domain (Table II). (3) At $P>P_c$, the strength data asymptotically approach the (flaw-size independent) limiting curve for true cones. The degradation is remarkably slight, considering the intensity of loading supported by the glass during indentation. However, above loads of 3 kN, the testing tended to end abruptly with sudden failure of either indenter or specimen.

Table II. Critical Loads to Cone Fracture, Computed from Eqs. (1) and (2) for Soda-Lime Glass for Given Indenter $r=1.58$ mm, as a Function of Flaw Size*

c_f^0 (μm)	23	19	16	12	10
P_c† (N)	0.4	0.5	0.7	1.0	1.4
P_c‡ (N)	390	390	390	390	390

*Note that P_c(Eq. (2))$>P_c$(Eq. (1)) for all c_f^0, i.e. data lie in the "Auerbach region" (see Fig. 2). †From Eq. (1). ‡From Eq. (2).

(B) Effect of Sphere Radius: A second set of tests was run to investigate the influence of indenter size. Data and theory are represented in Fig. 4 for an abrasion flaw size of 10 μm. The different regions of behavior are, as before: (1) At $P<P_c$, negligible degradation. (2) At $P=P_c$, the fall-off point scales with sphere radius, once more in accord with Auerbach behavior (Table III). (3) At $P>P_c$, an asymptotic approach to the limiting curve is again observed (this occurring more rapidly with diminishing indenter scale, with the smallest spheres producing a slight tendency to overshoot below the calculated curve). Again, the accumulation of data was limited by abrupt failure during indentation.

IV. Discussion

Within the limits of the assumptions in the Hertzian fracture model, the present analysis establishes a conservative basis for predetermining the strength properties of brittle ceramics in contact situations involving blunt indenters. In addition, it provides an indication as to which materials might be expected to suffer the least degradation. Thus, according to Eqs. (1) and (2), the onset of strength loss may be suppressed to a certain extent by choosing materials with large Γ and ν values (larger ν leading to smaller χ in Eq. (1) and to smaller ϕ in Eq. (2)[9]). Again, according to Eq. (5), the strength loss when degradation occurs may be minimized at large Γ (Γ being influenced by microstructure, e.g. grain size), large ν (a larger ν diminishing κ in Eq. (5)), and large E. That is, the material should be tough and stiff, with a large Poisson's ratio to restrain the development of high tensile stress in the indentation field.†

However, for a given indenter, the most practical means of controlling the prospective degradation is via the state of the brittle surface. As seen in Fig. 3, once c_f^0 is larger than the 10 μm typical of ceramic surfaces, it is not a sensitive factor in the reckoning of strength degradation. Indeed, if anything, the critical load for the onset of significant degradation is greater for the more severely abraded surfaces. This agrees with previous observations of the function P_c (c_f^0), as indicated by the experimental curve in Fig. 2; indeed, it seems that a 10-fold increase in flaw size can lead to a 2-fold increase in critical load in certain favorable cases.[9] Although such behavior may be contrary to intuitive expectation, a logical explanation is to be found in the very factor responsible for the Auerbach relation (Eq. (2)), i.e. the inhomogeneous nature of the Hertzian field. Basically, for very large flaws (typically, $c_f^0\gtrsim0.1a$) the stress gradients in the indentation field can reach the point where the component of normal stress along the flaw length actually changes from tensile at the surface to compressive below the surface[9]; such flaws will accordingly propagate less easily than smaller flaws contained entirely within the region of complete tension near the indented surface. This result is interesting in that it suggests

*As indicated in Section II, it is possible to compute values of these dimensionless constants directly from a knowledge of the Hertzian elastic stress field, using basic fracture mechanics. However, the degree of uncertainty in absolute values thus computed is currently such that direct experimental calibration affords, by far, the more reliable data (Ref. 1).

†At the limiting value $\nu=0.5$, the tensile component in the general indentation field disappears altogether (Ref. 16).

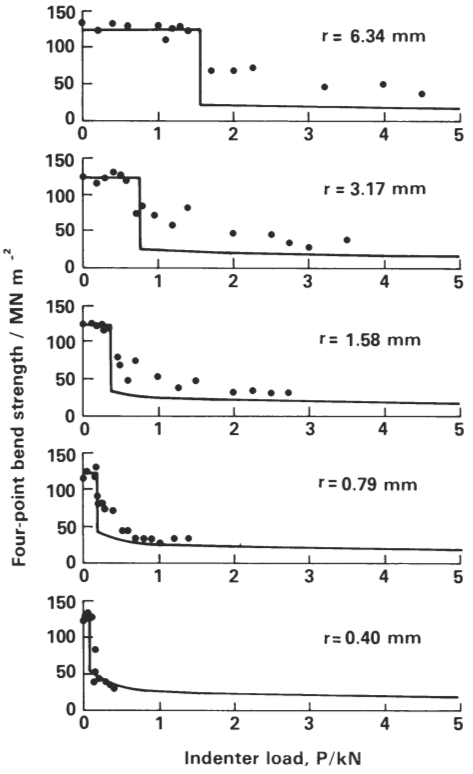

Fig. 4. Strength degradation as a function of indentation load, for soda-lime glass surfaces containing given abrasion flaws, $c_f^0 = 10\ \mu$m, using tungsten carbide spheres of different radii (indicated). Oil environment. Crosshead speed for indentation tests was 0.5 mm min^{-1}, for bend tests, 50 mm min^{-1}.

Table III. Critical Loads to Cone Fracture for Soda-Lime Glass for Given Flaw Size $c_f^0 = 10\ \mu$m, as Function of Indenter Radius*

r (mm)	6.34	3.17	1.58	0.79	0.40
P_c(Eq. (1)) (N)	22	5.5	1.4	0.3	0.1
P_c(Eq. (2)) (N)	1560	780	390	195	98.5

*Note that P_c(Eq. (2)) > P_c(Eq. (1)) for all r, i.e. data lie in "Auerbach region."

deliberate, severe preabrasion treatment as a potential means of inhibiting the onset of degradation. (At the same time, however, such treatment would, of course, weaken the material in flexure, etc.)

The present analysis, although quasi-static, may be usefully extrapolated to certain time-dependent contact situations. Impact-induced damage is an important practical case in point. Here, the quasi-static approximation should hold, provided the rate of contact does not approach the velocity of elastic waves. The impact conditions under which such an extrapolation may be made are currently under investigation. The advantages of using characteristic indentation fracture parameters obtained in simple hardness testing routines to predict more complex phenomena involving in-service damage events are self-evident. Once the velocity of projectile impingement approaches sonic values, the problem becomes a dynamic one, and the present analysis becomes invalid.

There are other time-dependent features in cone crack growth which further complicate the general description. In particular, the consideration of complex, nonequilibrium crack configurations has been avoided. Kinetic crack extension can occur in a wide range of ceramic materials, notably as a result of crack-tip interactions with hostile environments. This is especially true of silicate glasses, where ambient moisture causes subcritical cracks to propagate at substantial velocities (typically, up to 1 mm s^{-1}).[17] The present procedure of placing a thin film of oil on the abraded glass surfaces to restrict the access of moisture to the cracks therefore limits the range of applicability of the calculations in their present state. Nevertheless, some of the most important practical degradation situations would appear to be sufficiently well simulated in the present experimental arrangement, e.g. the case of impact in which the duration of contact is too brief for environmental effects to manifest themselves, and operations under inert or vacuum condition (e.g. spacecraft).

When the present results are related to practical problems, one must consider the history of a ceramic component, subsequent to any contact event. Indentation-induced cracks are susceptible to mechanical or thermal shock; stepwise repropagations can occur, thereby enlarging apparently innocuous cracks to potentially dangerous dimensions.[18] On the other hand, some cracks may actually close up and heal, either spontaneously, if sufficiently fast-running that contaminants do not penetrate along the interface, or via mass transport at high temperatures.[18,19]

One further point needs to be emphasized. As mentioned in Section III (2), the glass test pieces were prone to sudden failure at high indentation loads (i.e. if the spherical indenter did not fail first). An examination of indented surfaces invariably revealed a pattern of radial cracks extending outward from the contact center just before failure. This was especially noticeable for the smaller indenters; indeed, in the case of the sphere of $r = 0.40$ mm in Fig. 4, radial cracking was evident at loads not much in excess of the critical value for cone formation and appeared to be associated with a slight tendency for the data points to overshoot the predicted degradation curve. Such radial crack patterns are more typical of sharp indenters. Evidently, at suitably high loads small spheres are capable of producing irreversible flow in the material, and, thus, of penetrating the surface[1]; this is aided by the fact that the expanding contact area tends to encompass the surface trace of the cone crack at higher loads and, thereby, to suppress further cone extension. Since this alternative crack system is potentially more degrading than the cone crack system, it demands closer examination. This will be the topic of the second paper in the present study.

The strength degradation curves described herein for indentation damage are somewhat similar to those described by Hasselman[20] for thermal shock. In both cases there exists a range of "loading" (i.e. a load-range limit, ΔP, or temperature range, ΔT) over which little, if any, degradation is apparent. At a critical load, both descriptions imply an abrupt decrease in strength followed by a more gradual decrease with any further load increase. A common feature of the indentation and thermal shock situations at subcritical loading is that the available strain energy is insufficient for unstable crack propagation. The condition for ultimate crack arrest once a supercritical condition has been exceeded is, however, somewhat different for the 2 cases, being caused by a rapid (approximately inverse-square) decrease in the stress field around the contact point during indentation, and to the fixed-grip nature of the loading in thermal shock. Further differences also arise from the somewhat different means of initiating surface flaws in the 2 cases.

APPENDIX

The mode of failure of a cone-shaped crack in a uniform tensile stress field has been given only cursory consideration.[2] Full-scale fracture is expected to initiate from one of two diametrically opposite positions on the base rim of the cone coincident with the symmetry plane containing the axes of initial contact loading and subsequent flexural tension. An approximate solution for this configuration may be obtained by disregarding the crack curvature on either side of any such favored position, considering, instead, the representative case of a plane crack of half-length C, infinity width (parallel to the crack front), and an inclination α to the tensile axis. The scheme is shown in Fig. A1.

Now standard fracture-mechanics procedures can be applied to the problem.[21] The stress-intensity factors for an inclined-plane crack in uniform tension are

$$K_I = \sigma(\pi C)^{1/2} \sin^2 \alpha$$
$$K_{II} = \sigma(\pi C)^{1/2} \sin \alpha \cos \alpha \qquad \text{(A1)}$$

where the subscripts denote *I*, opening, and *II*, sliding, modes of fracture. (Actually, since the present representative configuration involves only an edge crack, an additional multiplying factor of

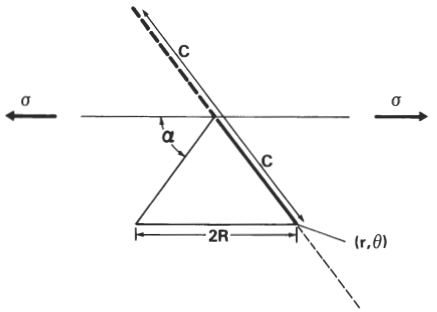

Fig. A1. Plane-crack representation of Hertzian cone configuration (side view). The crack increment at (r,θ) with respect to the origin of the tip of the representative crack is sought; this optimizes energy-release conditions.

≈ 1.12 should appear on the right side of the expressions in Eq. (A1).[20] However, this factor is somewhat nullified by a further factor (<1) arising from the curvature in the cone crack situation.) The present problem is complicated by the fact that the crack will not, in general, extend in its own plane; rather, it will tend to extend at some energetically favorable tilt angle θ, as indicated in Fig. A1. This complication can be handled by regarding the critical incremental extension as a reinitiation process in the near field of the original crack.[22] Note that the incremental crack experiences both opening and sliding types of local stress:

$$\sigma_{\theta\theta}=[K_I/(2\pi r)^{1/2}]f_{\theta\theta}{}^{I}+[K_{II}/(2\pi r)^{1/2}]f_{\theta\theta}{}^{II}=K_I'/(2\pi r)^{1/2}$$
$$\sigma_{r\theta}=[K_I/(2\pi r)^{1/2}]f_{r\theta}{}^{I}+[K_{II}/(2\pi r)^{1/2}]f_{r\theta}{}^{II}=K_{II}'/(2\pi r)^{1/2} \quad \text{(A2)}$$

where the f terms are the angular-dependent components of the standard crack-tip stress formulas,[21,22]

$$\left.\begin{aligned} f_{\theta\theta}{}^{I}&=\cos^3(\theta/2)\\ f_{r\theta}{}^{I}&=\sin(\theta/2)\cos^2(\theta/2)\end{aligned}\right\} \quad \text{(mode } I\text{)} \quad \text{(A3)}$$

$$\left.\begin{aligned} f_{\theta\theta}{}^{II}&=-3\sin(\theta/2)\cos^2(\theta/2)\\ f_{r\theta}{}^{II}&=\cos(\theta/2)[1-3\sin^2(\theta/2)]\end{aligned}\right\} \quad \text{(mode } II\text{)} \quad \text{(A4)}$$

and the "transformed stress-intensity factors" K_I' and K_{II}' defined the field for the modified crack. Equations (A2) and (A1) give

$$K_I'(\theta,\alpha)=\sigma(\pi C)^{1/2}[(f_{\theta\theta}{}^{I}\sin^2\alpha)+(f_{\theta\theta}{}^{II}\sin\alpha\cos\alpha)]$$
$$K_{II}'(\theta,\alpha)=\sigma(\pi C)^{1/2}[(f_{r\theta}{}^{I}\sin^2\alpha)+(f_{r\theta}{}^{II}\sin\alpha\cos\alpha)] \quad \text{(A5)}$$

The most favorable path energetically from the original crack tip is determined by computing the mechanical-energy-release rate G/unit width of the crack front as a function of angular variation

$$G(\theta,\alpha)=[(1-\nu^2)/E][(K_I')^2(\theta,\alpha)+(K_{II}')^2(\theta,\alpha)] \quad \text{(A6)}$$

For a given inclination angle α, it may be assumed that for isotropic solids the crack will extend at that angle θ^* which gives a maximum $G^*(\alpha)$ in the energy release, i.e.

$$\partial G/\partial\theta=0 \quad \text{(A7)}$$

This equation, in conjunction with Eqs. (A5), (A4), and (A3), reduces Eq. (A6) to

$$G^*(\alpha)=[\pi(1-\nu^2)\sigma^2C/E]\omega(\alpha) \quad \text{(A8)}$$

where $\omega(\alpha)$ is a dimensionless constant which attains a limiting value (unity) for normal cracks.

Equation (A8) then leads directly to the strength equation (Eq. (4)) if the Griffith energy-balance condition

$$G^*=2\Gamma \quad \text{(A9)}$$

is satisfied and if

$$c_f=C\omega(\alpha) \quad \text{(A10)}$$

is written as the effective length of the flaw. In the limit of well-developed cones ($R>>R_0$, Fig. 1),

$$C=R/\cos\alpha \quad \text{(A11)}$$

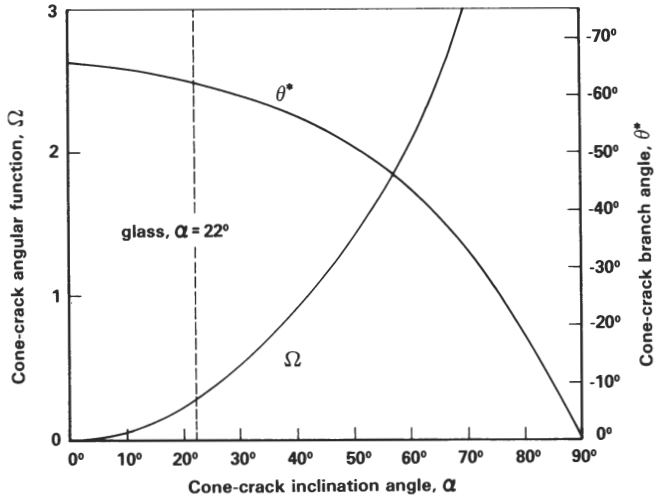

Fig. A2. Angular terms for cone-crack extension in tensile field.

Thus, from Eqs. (A10) and (A11),

$$c_f/R=\omega(\alpha)/\cos\alpha\equiv\Omega(\alpha) \quad \text{(A12)}$$

The quantity $\Omega(\alpha)$, therefore, defines our required angular term in Eq. (5) of the text. Both Ω and θ^* (evaluated numerically) are plotted in Fig. A2. For the special case of $\alpha=22°$ (glass), values for Ω and θ^* are computed as 0.25 and $-63°$, respectively. An independent, empirical evaluation from strength data by Evans[2] yields $\Omega=0.20$. Since Ω ultimately appears in the degradation formula (Eq. (5*b*)) under a square root, uncertainties in the above analysis will not be of major significance.

Acknowledgments: The writers are indebted to A. G. Evans for motivating discussions in the early stages of this work, and to E. R. Fuller for assistance throughout.

References

[1] B. R. Lawn and T. R. Wilshaw, "Indentation Fracture: Principles Applications," *J. Mater. Sci.*, **10** [6] 1049–81 (1975).
[2] A. G. Evans, "Strength Degradation by Projectile Impacts," *J. Am. Ceram. Soc.*, **56** [8] 405–409 (1973).
[3] F. C. Frank and B. R. Lawn, "Theory of Hertzian Fracture," *Proc. Roy. Soc., London, Ser. A*, **299** [1458] 291–306 (1967).
[4] B. R. Lawn, "Hertzian Fracture in Single Crystals with the Diamond Structure," *J. Appl. Phys.*, **39** [10] 4828–36 (1968).
[5] F. B. Langitan and B. R. Lawn, "Hertzian Fracture Experiments on Abraded Glass Surfaces as Definitive Evidence for an Energy Balance Explanation of Auerbach's Law," *J. Appl. Phys.*, **40** [10] 4009–17 (1969).
[6] T. R. Wilshaw, "Hertzian Fracture Test," *J. Phys. D*, **4** [10] 1567–81 (1971).
[7] A. G. Mikosza and B. R. Lawn, "Section-and-Etch Study of Hertzian Fracture Mechanics," *J. Appl. Phys.*, **42** [13] 5540–45 (1971).
[8] J. S. Nadeau, "Hertzian Fracture of Vitreous Carbon," *J. Am. Ceram. Soc.*, **56** [9] 467–72 (1973).
[9] B. R. Lawn, T. R. Wilshaw, and N. E. W. Hartley, "Computer Simulation Study of Hertzian Cone Crack Growth," *Int. J. Fract. Mech.*, **10** [1] 1–16 (1974).
[10] F. C. Roesler, "Brittle Fractures Near Equilibrium," *Proc. Phys. Soc., London, Sect. B*, **69** [10] 981–92 (1956).
[11] A. A. Griffith, "Phenomena of Rupture and Flow in Solids," *Phil. Trans. Roy. Soc. (London), Ser. A*, **221** [4] 163–98 (1920).
[12] F. Auerbach, "Measurement of Hardness," *Ann. Phys. Chem.*, **43**, 61 (1891).
[13] R. E. Mould and R. D. Southwick, "Strength and Static Fatigue of Abraded Glass Under Controlled Ambient Conditions: I," *J. Am. Ceram. Soc.*, **42** [11] 542–47 (1959).
[14] R. E. Mould and R. D. Southwick, "Strength and Static Fatigue of Abraded Glass Under Controlled Ambient Conditions: II," *ibid.*, pp. 582–92.
[15] S. M. Wiederhorn, "Fracture Surface Energy of Glass," *ibid.*, **52** [2] 99–105 (1969).
[16] B. R. Lawn and M. V. Swain, "Microfracture Beneath Point Indentations in Brittle Solids," *J. Mater. Sci.*, **10** [1] 113–22 (1975).
[17] S. M. Wiederhorn, "Influence of Water Vapor on Crack Propagation in Soda-Lime Glass," *J. Am. Ceram. Soc.*, **50** [8] 407–14 (1967).
[18] S. M. Wiederhorn, B. J. Hockey and D. E. Roberts, "Effect of Temperature on the Fracture of Sapphire," *Phil Mag.*, **28** [4] 783–95 (1973).
[19] B. J. Hockey and B. R. Lawn, "Electron Microscopic Observations of Microcracking About Indentations in Aluminum Oxide and Silicon Carbide," *J. Mat. Sci.*, **10**, 1275–84 (1975).
[20] D. P. H. Hasselman, "Unified Theory of Thermal Shock Fracture Initiation and Crack Propagation in Brittle Ceramics," *J. Am. Ceram. Soc.*, **52** [11] 600–604 (1969).
[21] P. C. Paris and G. C. Sih, "Stress Analysis of Cracks," *Am. Soc. Test. Mater., Spec. Tech. Publ.*, No. **381**, 30–83 (1965).
[22] B. R. Lawn and T. R. Wilshaw, Fracture of Brittle Solids; Chapter 3. Cambridge University Press, London, 1975.